Differential Localization and Functional Role of Calsequestrin in Growing and Differentiated Myoblasts

Martha Raichman, Maria Carla Panzeri, Emilio Clementi,* Panagiota Papazafiri, Mark Eckley,‡ Dennis O. Clegg,‡ Antonello Villa, and Jacopo Meldolesi

Department of Pharmacology, CNR Molecular and Cellular Pharmacology and B. Ceccarelli Centers, and Dipartimento di Ricerca Biologica e Tecnologica, Scientific Institute San Raffaele, University of Milano, 20132 Italy; *Chair of Pharmacology, Faculty of Pharmacy, University of Reggio Calabria, Catanzaro, 88021 Italy; and ‡Neuroscience Research Institute, Division of Molecular, Cellular and Developmental Biology, Department of Biological Sciences, University of California, Santa Barbara, California 93106

Abstract. Calsequestrin (CSQ) is the low affinity, high capacity Ca^{2+}-binding protein concentrated within specialized areas of the muscle fiber sarcoplasmic reticulum (a part of the ER) where it is believed to buffer large amounts of Ca^{2+}. Upon activation of intracellular channels this Ca^{2+} pool is released, giving rise to the $[Ca^{2+}]_i$ increases that sustain contraction. In order to investigate the ER retention and the functional role of the protein, L6 rat myoblasts were infected with a viral vector with or without the cDNA of chicken CSQ, and stable clones were investigated before and after differentiation to myotubes. In the undifferentiated L6 cells, expression of considerable amounts of heterologous CSQ occurred with no major changes of other ER components. Ca^{2+} release from the ER, induced by the peptide hormone vasopressin, remained however unchanged, and the same occurred when other treatments were given in sequence to deplete the ER and other intracellular stores: with the Ca^{2+} pump blocker, thapsigargin; and with the Ca^{2+} ionophore, ionomycin, followed by the Na^+/H^+ ionophore, monensin. The lack of effect of CSQ expression on the vasopressin-induced $[Ca^{2+}]_i$ responses was explained by immunocytochemistry showing the heterologous protein to be localized not in the ER but in large vacuoles of acidic content, positive also for the lysosomal enzyme, cathepsin D, corresponding to a lysosomal subpopulation. After differentiation, all L6 cells expressed small amounts of homologous CSQ. In the infected cells the heterologous protein progressively decreased, yet the $[Ca^{2+}]_i$ responses to vasopressin were now larger with respect to both control and undifferentiated cells. This change correlated with the drop of the vacuoles and with the accumulation of CSQ within the ER lumen, where a clustered distribution was observed as recently shown in developing muscle fibers. These results provide direct evidence for the contribution of CSQ, when appropriately retained, to the Ca^{2+} capacity of the rapidly exchanging, ER-located Ca^{2+} stores; and for the existence of specific mechanism(s) (that in L6 cells develop in the course of differentiation) for the ER retention of the protein. In the growing L6 myoblasts the Ca^{2+}-binding protein appears in contrast to travel along the exocytic pathway, down to post-Golgi, lysosome-related vacuoles which, based on the lack of $[Ca^{2+}]_i$ response to ionomycin-monensin, appear to be incompetent for Ca^{2+} accumulation.

ACCUMULATION of Ca^{2+} within the cisternae of the ER is a general property of eukaryotic cells. A family of pumps, the sarcoplasmic-endoplasmic reticulum Ca^{2+} ATPases (SERCAs),[1] takes care of the transport of the cation across the membrane, and various lumenal proteins are responsible for its low affinity binding and storage. This last activity keeps the free lumenal concentration of the cation at a level (most probably in the 10^{-3}–10^{-4} M range) requested by local ER functions (Pozzan et al., 1994). In addition, the segregated pool remains rapidly releasable in case the channels present in the ER limiting membrane are activated (see Berridge, 1993; Pozzan et al., 1994).

Among the lumenal Ca^{2+}-binding proteins, two are be-

Address all correspondence to Prof. J. Meldolesi, DIBIT, Sci. Institute S. Raffaele, Via Olgettina, 58, 20132 Milano, Italy. Tel.: (39) 2 26432770. Fax: (39) 2 26434813.

1. *Abbreviations used in this paper*: Ab, antibody; BSA, bovine serum albumin; $[Ca^{2+}]_i$, cytosolic Ca^{2+} concentration; CatD, cathepsinD; CR, calreticulin; CSQ, calsequestrin; DAMP, 3-(2,4-Dinitroanilino)-3′amino-*N*-methyldipropylamine; SR, sarcoplasmic reticulum; GC, Golgi complex; IP_3, inositol 1,4,5 trisphosphate; SERCA, sarcoplasmic-endoplasmic reticulum Ca^{2+}-ATPase; PDI, protein disulfide isomerase; Tg, thapsigargin; Vp, vasopressin.

lieved to play a major role in the storage of the cation. Calreticulin (CR) appears to be ubiquitously expressed, although its levels are often variable depending also on the differentiation state of the cell. Within the ER lumen CR is widely distributed, similar in this respect to other resident proteins (Michalak et al., 1992; Pozzan et al., 1994). Calsequestrin (CSQ), on the other hand, is expressed by only a few cell types, especially muscle fibers. Fast twitch skeletal muscles express a first (Fliegel et al., 1987) and the heart a second (Scott et al., 1988) isoform, while slow twitch and various smooth muscles can express both (Volpe et al., 1994). Outside muscles, CSQ expression has been reported only in the Purkinje neurons of birds (Volpe et al., 1990). On simple functional and molecular grounds CSQ appears to resemble CR by a variety of criteria. It has approximately the same relative molecular weight and binds Ca^{2+} with approximately the same low affinity (k_D ~1 mM) and high stoichiometry (1/25–50). The general organization of the two proteins, with a highly acidic Ca^{2+}-binding COOH-terminal domain, is also similar (Fliegel et al., 1987; Michalak et al., 1992; Pozzan et al., 1994). However, profound differences exist in the amino acid sequence. In particular, CSQ does not exhibit at its very COOH terminus the tetrapeptide KDEL (Fliegel et al., 1986; Scott et al., 1988) recognized by the recycling receptor which unables CR and several other proteins to maintain their ER lumenal localization (Pelham, 1988). Moreover, the distribution of CSQ is not even throughout the lumen but is markedly concentrated into discrete areas (e.g., the terminal cisternae of the skeletal muscle sarcoplasmic reticulum [SR]), localized in close proximity to the release channels, the ryanodine, and/or inositol 1,4,5-trisphosphate (IP_3) receptors (Franzini-Armstrong et al., 1987; Villa et al., 1993*a*; Pozzan et al., 1994). These discrete areas appear therefore specialized to assure the high efficacy of two coordinate processes: on the one hand, Ca^{2+} storage; on the other hand, Ca^{2+} release from the ER lumen to the surrounding cytosol.

During the last several years, the peculiar localization of CSQ has attracted considerable interest, however the underlying mechanisms have not been fully identified yet. Electron microscopy studies have revealed the protein to be arranged into dense, apparently insolubilized masses visible already during early postnatal steps of skeletal muscle development (Flucher, 1992; Villa et al., 1993*b*). These masses, which initially appear randomly scattered throughout the entire ER, progressively concentrate into the specialized discrete areas observed in the adult, apparently attached to the lumenal surface of the membrane by discrete filaments possibly composed by integral membrane proteins protruding into the lumen (Franzini-Armstrong et al., 1987). Up until now, however, the information about the filaments or other anchorage mechanisms of the CSQ masses has not gone much beyond description and hypotheses (Mitchell et al., 1988; Damiani and Margreth, 1990; Knudson et al., 1993).

Because of its peculiar properties, CSQ can be envisaged as an interesting tool to investigate mechanisms that underlie the ER structure and function. The experimental approach that we have used was based on the expression in L6 cells, a line of rat myoblasts, of a heterologous form of the protein, specific of chicken muscles (Clegg et al., 1988; Choi and Clegg, 1990). In their undifferentiated, growing state the cells of this line exhibit a fibroblast-like phenotype which turns towards muscle differentiation, with expression of specific markers including CSQ, only after a few-day culture into a low-serum medium (Yaffe, 1968, 1973). Stable clones of these cells, infected either with or without the cDNA for the chicken muscle Ca^{2+}-binding protein, were studied both before and after differentiation by a comprehensive approach that included biochemistry, physiology and immunocytochemistry. Our results have revealed new aspects of the cell biology of the CSQ protein with ensuing insights into the processes of Ca^{2+} distribution and Ca^{2+} homeostasis in eukaryotic muscle and nonmuscle cells.

Materials and Methods

Materials

The L6 myogenic cell line, described by Yaffe (1968), was purchased from American Type Culture Collection (Rockville, MD); fura-2, monensin, and ionomycin from Calbiochem-Behring Corp. (San Diego, CA); thapsigargin (Tg) from L.C. Service Corp. (Woburn, MA). The antibodies (Abs) used have been described elsewhere: anti-CSQ, a rabbit polyclonal Ab, by Hall et al. (1988); anti-CR, a rabbit polyclonal Ab, by Perrin et al. (1991); anti-ER membrane proteins, affinity-purified rabbit polyclonal Abs, by Louvard et al. (1982); anti-bovine protein disulfide isomerase (PDI), a rabbit polyclonal Ab, by Villa et al. (1993*a*); anti-PDI C terminal tail (1D3) a mouse monoclonal Ab, by Vaux et al. (1990); anti-SERCA, a mouse monoclonal Ab, by Colyer et al. (1989); anti-IP_3 receptors, a rabbit polyclonal Ab, by Peng et al., 1991; anti-cathepsin D (catD), a rabbit polyclonal Ab, by Hashimoto et al., 1988. Rhodamine- and fluoresceine-labeled donkey IgGs against rabbit and mouse IgGs as well as rhodamine-labeled sheep IgGs against the same antigens, unlabeled goat Fab fragments and goat serum were purchased from Technogenetics (Milan, Italy). Colloidal gold particles (5 and 15 nm), coated with goat IgGs against either rabbit (large and small particles) or mouse (small particles only) IgGs, were purchased from Biocell (Cardiff, UK). Before each labeling experiment the colloidal gold preparations were carefully checked in the electron microscope for adherence to specifications in terms of both size uniformity and absence of aggregates. Only the preparations exhibiting >95% of single particles and no aggregates larger than two particles were used in the present work. Other chemicals were analytical or the highest grade available. [^{125}I]Protein A and the sheep anti-mouse [^{125}I] mAb were purchased from Amersham Int. (Buckinghamshire, England); 3-(2,4-Dinitroanilino)-3'amino-*N*-methyldipropylamine (DAMP) and anti-DAMP Ab from Oxford Biomedical Research (Oxford, MI); culture sera and media from GIBCO (Basel, Switzerland); glass microfiber filters from Whatman, (Maidstone, U.K.); the remaining chemicals from Sigma-Aldrich (Milan, Italy).

Generation and Growth of Cell Clones

Construction of retroviral expression vectors containing the *neo*-gene, with or without the chicken CSQ cDNA (Clegg et al., 1988) inserted behind a human cytomegalovirus intermediate early promoter/enhancer, has been described in Muller et al. (1990). Plasmid DNA was purified from *Escherichia coli* strain DH5-α by the alkaline SDS lysis–CsCl gradient procedure (Sambrook et al., 1989) and infected into the retroviral packaging cell line PA317 (Bender et al., 1987) using the cationic lipid lipofectin (Bethesda Research Labs, Bethesda, MD) (Muller et al., 1990). Various separate G418-resistant clones were isolated and expanded, and tissue culture supernatants from confluent cultures (Bender et al., 1987) were cleared of debris by centrifugation at 3,000 *g* and used to infect L6 cells.

For infection, L6 cells were cultured for 24 h in DME containing 20% FCS and 400 μg/ml polybrene, in the presence of varying dilutions of viral particles. After washing away the polybrene and harvesting the cells, transductants were selected by growth in media containing 400 μg/ml active G418 (Geneticin; BRL-GIBCO, Bethesda, MD) for 14 d. Resistant colonies were subcloned by dilution and grown in 96-well plates. Selected derivatives of L6 were propagated into 10 cm Petri dishes in the presence of 400 μg/ml G418 to maintain selective pressure. Cells were fed every other day with high serum media (DME containing 20% FCS) and passed by trypzinization when 75% confluent.

Differentiation of myoblasts to myotubes was obtained according to the protocol described by Yaffe (1973). Briefly, myoblasts were plated onto 10

cm Petri dishes (2×10^6 cells/dish) previously coated with gelatin (0.01%) for 15 min at room temperature, in the above described culture medium. After 2 d of culture, cells were bathed in the differentiation medium containing DME, 2% horse serum, 0.04 U/ml insulin.

SDS-PAGE and Western Blotting

The various cell preparations were harvested, washed in PBS, and then lysed in 150 mM NaCl, 15 mM $MgCl_2$, 1 mM EGTA, 1 mM PMSF, 50 mM Hepes-KOH, 10% glycerol, 1% Triton X-100, pH 7.5. After addition of SDS and β mercaptoethanol, the samples were boiled and 50–80 μg of protein (measured by the bicinchonic acid procedure) were loaded into the slots of 10% SDS polyacrylamide minigels which were run as described elsewhere (Villa et al., 1992). High transfer of proteins onto nitrocellulose membranes was carried out at 200 mA for 18 h in a buffer containing: 25 mM Tris, 192 mM glycine, 20% methanol, pH 8.3. After transfer, both the gels and the blots were routinely stained with Ponceau red. Blots were processed at room temperature, first for 1 h with PBS + 3% BSA, then for 2 h with appropriate concentration of the specific Abs in the same buffer. After washing five times for 5 min with 150 mM NaCl, 50 mM Tris-HCl, 0.05% Tween-20, 5% powdered milk, pH 7.4, the blotted bands were decorated with [^{125}I]protein A. The blots were washed five times for 10 min with the above buffer, dried, and then finally autoradiographed at −80°C for variable periods of time. Quantitation of the various bands was obtained by microdensitometry in a Molecular Dynamics Imagequant apparatus. Results shown are representative of three to five separate experiments.

Secretion Studies

For secretion studies, the proteins present in the culture media were precipitated by adding solid ammonium sulfate at 80% saturation, and the suspensions were stirred for 30 min. The pH was then adjusted to 4.7 with phosphoric acid and the suspensions were stirred for more than 4 h in the cold room. The precipitated proteins were collected by centrifugation at 15,000 *g* for 20 min, the pellet was dissolved, dialyzed against PBS, and finally analysed on 10% SDS polyacrylamide minigels as described in the preceding section.

$[Ca^{2+}]_i$ Measurements

At the beginning of the experiments, the differentiated and undifferentiated cell preparations were harvested, washed, and finally loaded for 30 min at 37°C (while suspended in DME containing either 10 or 2% FCS: undifferentiated or differentiated cells, respectively) with the Ca^{2+} sensitive dye fura-2, added as acetoxymethylester (final concentration, 5 μM). Cells were then diluted in Krebs Ringer Hepes medium containing: 125 mM NaCl, 5 mM KCl, 1.2 mM KH_2PO_4, 1.2 mM $MgSO_4$, 2 mM $CaCl_2$, 6 mM glucose, 25 mM Hepes-NaOH, pH 7.4, to a final concentration of 3–4 $\times$ 10^6 cells/ml, and kept at 37°C until use. Cell aliquots (4×10^6 cells) were centrifuged, resuspended by gentle swirling in 1.5 ml of medium supplemented with 250 μM sulfinpyrazone (to prevent dye leakage), and finally transferred to a thermostatted cuvette (37°C) maintained under continuous stirring in a fluorimeter (LS-5B; Perkin Elmer Corp., Eden Prairie, MN). Analyses were carried out as recommended by Grynkiewicz et al. (1985). 1 min before adding the Ca^{2+} releasing agents, the samples were supplemented with excess EGTA (3 mM; Ca^{2+}-free medium). Results are shown as traces and graphs. Traces are representative of the results obtained in at least eight separate experiments; graphs show the average values ± SD of 3–12 experiments.

Conventional and Immuno Microscopy

Cell culture monolayers were fixed in situ for 2 h at 4°C with 4% paraformaldehyde, 0.25% glutaraldehyde in 125 mM phosphate buffer, and then washed with the buffer. Some monolayers were processed for immunofluorescence as such, others were detached by scratching, suspended in the phosphate buffer, and centrifuged at low speed. The pellets thus obtained to be used for conventional electron microscopy were washed extensively with phosphate buffer, postfixed with 1% OsO_4 in 125 mM cacodylate buffer, dehydrated in ethanol, block stained with uranyl acetate, and embedded in Epon. Thin sections were doubly stained with uranyl acetate and lead citrate. Samples for cryosections were infiltrated with concentrated sucrose, frozen in a 3:1 (vol/vol) mixture of propane and cyclopentane cooled with liquid nitrogen, and transferred to an ultramicrotome TOP 170A with a cryosection apparatus TOP CRYO 200 (Pabisch, W., S.p.A., Milan, Italy). The sections for immuno fluorescence (~1-μm thick, flattened over glass slides) as well as the fixed monolayers were covered with 2% liquid gelatin in 125 mM Na phosphate buffer, pH 7.4. After a short treatment with 1% Na borohydrate (to eliminate glutaraldehyde fluorescence) they were washed and exposed for 30 min to a solution containing 0.3% Triton X-100, 15% filtered goat serum, 0.45 M NaCl, and 10 mM phosphate buffer, pH 7.4. After washing, the sections were exposed (1 h at 37°C or overnight at 4°C) to any one of the various primary Abs diluted in the above Triton X-100 and goat serum-containing solution. They were then washed thoroughly and treated with the appropriate rhodamine-labeled sheep Abs (1:20–1:40 in the Triton X-100, goat serum solution, 30–60 min, 37°C), washed again, and mounted in glycerol to be examined in either a Zeiss Photomicroscope III apparatus or a LSM Zeiss confocal scanning microscope (Carl Zeiss, Inc., Oberkochen, Germany), where images were recorded using a Focus Imagecorder Plus (Focus Graphics Inc., Foster City, CA). Controls in which the primary Ab was either omitted or replaced by preimmune or nonimmune IgGs yielded completely negative results. Dual labeling was carried out by sequential exposure of the samples to two Abs, revealed by rhodamine and fluoresceine, respectively, using precautions to prevent cross-labeling, signal spill-over, and bleed-through artifacts as described in detail by Villa et al. (1993*a*).

For immunogold labeling, ultrathin cryosections (50–100-nm thick) were collected over nickel grids and covered with 2% gelatin. After treatment with 125 mM Na phosphate buffer, pH 7.4, supplemented with 0.1 M glycine, they were exposed for 1 h at 37°C to the first Ab diluted in phosphate-glycine buffer, and then washed with the buffer and decorated with anti-IgG-coated gold particles (5 or 15 nm, dilution 1:80 in the same buffer). For dual labeling the sections were exposed in sequence to the two Abs followed by the corresponding gold particles, with appropriate washing and quenching steps in between (see Villa et al., 1993*a*). In all cases the anti-CSQ Ab and the large gold particles were applied second. The immunodecorated grids were then processed as recommended by Keller et al. (1984). Both conventional sections and cryosections were examined in a Hitachi H-7000 electron microscope. Pictures were usually taken at a magnification of 24,000.

With nonimmune serum, the 5 nm gold particle labeling was low and uniformly distributed over the cell nucleus and cytoplasm. The average labeling, calculated under standard conditions in a group of randomly chosen pictures, i.e., the background, was three to five gold particles/μm^2. With 15 nm particles the background values were variable, depending on the experimental conditions used (in no case >35 particles/μm^2). When the specific Abs were used, labeling over some cell structures, such as nuclei and mitochondria, was not significantly different from the background.

Results

Stable clones of rat L6 cells were selected (by G418 exposure) from the cell populations previously infected with constructs containing the retroviral expression-antibiotic resistance vector, with or without the cDNA of the chicken CSQ. The latter protein is known to run in SDS gels at a rate similar to the mammalian cardiac CSQ (52 kD; Choi and Clegg, 1990), and to be therefore easily distinguished in Western blots from the skeletal muscle isoform endogenously expressed by L6 cells after differentiation, which exhibits an apparent molecular weight 10 kD higher.

Protein Expression

A first series of experiments was carried out to characterize protein expression in control and CSQ-infected clones of L6 cells while in their fully growing, undifferentiated state. The results obtained are summarized in Figs. 1 and 2. Western blots obtained with total homogenates of two control and four CSQ-infected clones investigated for the two Ca^{2+}-binding proteins, CSQ and CR, are shown in Fig. 1. Expression of CR (Fig. 1 *B*) was found to be quite constant in all these clones. The values of this protein, established in this and in three additional experiments by microdensitometry in comparison with scale amounts of an authentic standard run in parallel (not shown), were found to vary between 1.5 and

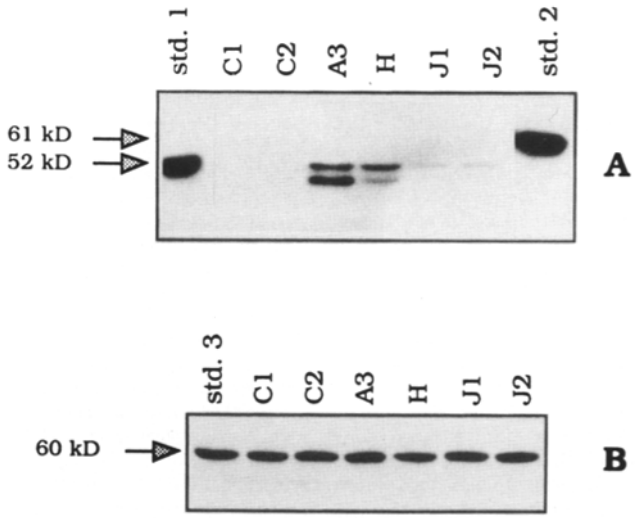

Figure 1. Western blot analysis for CSQ and CR in control (*C1* and *C2*) and CSQ-infected (*A3*, *H*, *J1*, and *J2*) L6 cell clones. *A* illustrates the Western blot labeling of CSQ. The two standards (*std. 1* and *std. 2*) are of rabbit heart and skeletal muscle CSQ, respectively. Notice that control clones are completely negative whereas of the infected clones two (*A3* and *H*) exhibit a prominent CSQ-positive doublet (~52 and 48 kD), the other two (*J1* and *J2*) a faint band running as the higher band of that doublet and as the heart standard. *B* shows CR Western blots, with the specific standard (*std. 3*). Notice that in all the clones the CR bands run the same and look very similar in intensity.

1.8 μg/mg of total homogenate protein. The CSQ results of the same clone homogenates are illustrated in Fig. 1 *A*. As can be seen, the two control clones, C1 and C2, exhibited immunoreactive bands neither at 52 nor at 61 kD, the positions of the infected and endogenous CSQ, respectively. In all the four CSQ-infected clones, on the other hand, immunodecorated bands positioned at 52 kD were clearly visible, although quite variable. In the two richest clones, A3 and H, a second CSQ-positive band appeared at the apparent molecular weight of 48 kD, whereas in the two poor clones, J1 and J2, clear second bands were never observed, even when exposure of the immunoblots was prolonged to obtain signal intensities comparable to those shown for the A3 and H clones. The actual CSQ values of the last two clones were measured by microdensitometry (as specified above for CR) in a total of 12 experiments. For the authentic band the results obtained varied between 1.1 and 1.5, for the faster band between 0.6 and 1.8 μg/mg of total homogenate protein. Overall, these levels of expression are comparable to those of normal skeletal muscle fibers (see Pozzan et al., 1994).

The Western blot characterization of homogenates of the two control and the two CSQ-rich clones, A3 and H, in their undifferentiated state, was pursued by the study of various other proteins known to play important roles in Ca^{2+} homeostasis (Fig. 2). In all clones, the anti-SERCA Ab revealed two bands at ~110 and 95 kD, probably corresponding to the 2b and 2a isoforms of the ATPase, respectively. Some differences of these bands were revealed among the clones, in particular C1 appeared rich in the lower band and H in both. These differences, however, might not be of great physiological significance since, with respect to the L6 cell mixed population and to other cell lines (not shown), all of the clones appeared well equipped with these pumping enzymes. Variability was observed also with two other proteins, however limited to moderate degrees (<30%): the intracellular Ca^{2+} channel, IP_3 receptor; and the lumenal enzyme, PDI, which is also a Ca^{2+}-binding protein (Fig. 2). Of the four main proteins recognized by the Ab raised against ER membranes (Louvard et al., 1982), the 91-kD calnexin and the low molecular weight, 28–29-kD proteins, previously described in other cell types, were found to be expressed at low levels in L6 cells. Two other bands, 66 (a doublet) and 48 kD, were more abundant, with some, but not major, heterogeneities among the clones (Fig. 2).

Further experiments were carried out with control and CSQ-infected cells induced to differentiate by low serum culturing (Yaffe, 1973). Fig. 3 illustrates the results obtained with CSQ and CR in the C1 and A3 clones. Similar results were obtained also with the C2 and H clones. CR was not consistently modified after 3 d. After 7 d, however, it was considerably decreased (−40–60% compared to undifferentiated cells; see also Opas et al., 1991) (Fig. 3 *B*). The changes in CSQ (Fig. 3 *A*) were more complex. First of all, the homologous skeletal isoform of the protein began to accumulate and was fully visible already after 7 d of differentiation. At later stages (10 and especially 20 d) the values in-

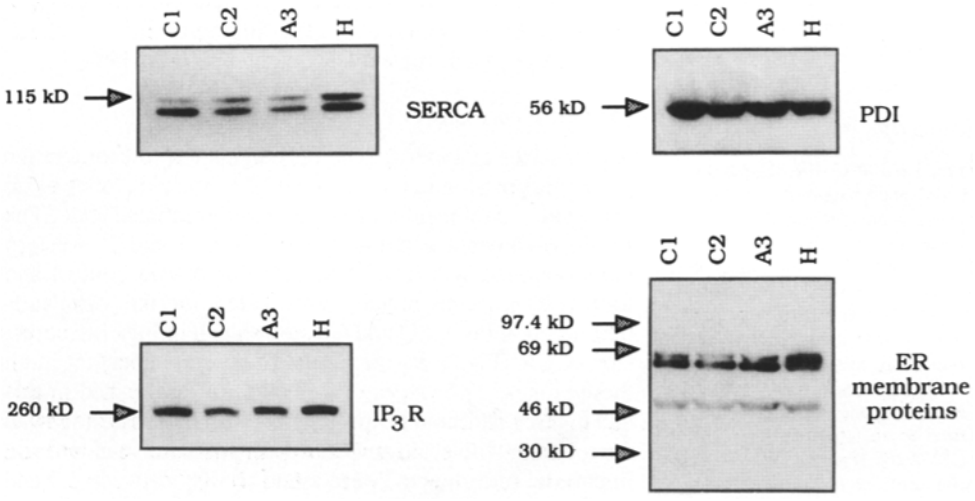

Figure 2. Western blot analysis for various ER components in control (*C1* and *C2*) and CSQ-infected (*A3* and *H*) L6 cell clones. Notice some variability among the clones in the expression of the SERCA pumps concerning in particular the more slowly running band. Expression of both the lumenal protein, PDI, and the IP_3 receptor (IP_3R) appears in contrast more even, while the anti-ER membrane protein blot reveals a doublet at 66 and a band at 48 kD, both moderately variable among the clones.

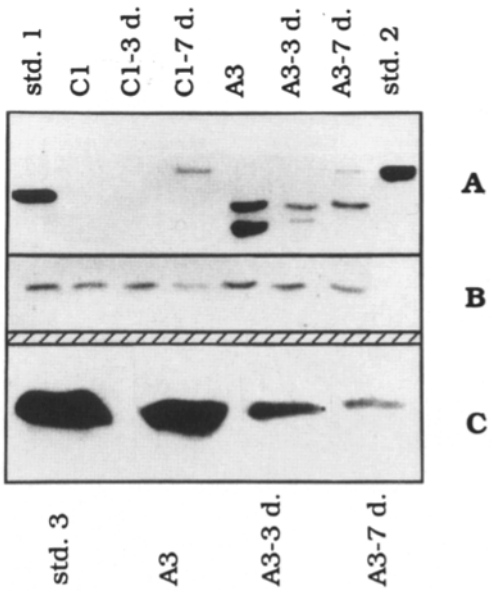

Figure 3. Western blot analysis for CSQ and CR of a control (*C1*) and a CSQ-infected (*A3*) L6 cell clone. In *A* and *B* the standards are positioned as in Fig. 1. *A* shows, to the left, the lack of homologous CSQ in control cells before and at 3-d differentiation, and the appearance of the protein at 7 d; to the right, the decreased expression of the heterologous Ca^{2+}-binding protein in the infected cells during differentiation (*3 d* and *7 d*), with appearance of the homologous protein, also at 7 d. *B* shows the decrease of CR at 7-d differentiation both in controls (*left*) and in CSQ-infected (*right*) cells. *C* shows the bands positive for heterologous CSQ revealed in the media bathing for 12 h the infected A3 cells at 0, 3, and 7 d of differentiation. The standard band to the left (*std. 3*) is of chicken CSQ. Compared to *A* and *B*, *C* was overexposed in order to reveal the 7-d band.

creased considerably (not shown). Concomitantly, the avian type protein decreased in the CSQ-infected cells, with a marked drop already at 3 d both of the authentic (−60%) and, especially, of the faster (−90%) CSQ-positive bands. At 7 d the faster band was no longer visible, while the authentic heterologous band stabilized at values only moderately higher than the homologous protein. Thereafter (10 and 20 d, not shown) the heterologous CSQ remained stable while the homologous protein increased, similar to the control cells.

CSQ immunoreactivity was also searched for in the incubation medium of the cells. The endogenous mammalian skeletal isoform was never detected, in both controls and CSQ-infected cells. In contrast, the avian form appeared in the medium of the CSQ-infected cells (~10% released in 12 h with respect to the total intracellular levels), however only as a single band of authentic relative molecular weight. The lower molecular weight CSQ band was never detected in the medium (Fig. 3 *C*). During differentiation the medium band decreased considerably, especially at 7 d (Fig. 3 *C*) and thereafter (not shown). In a few experiments, CSQ-infected A3 cells, before and after differentiation, were incubated in vitro for 2 h with the Ca^{2+} ionophore, ionomycin, 0.5 μM. In other cell types this treatment has been shown to greatly increase the rate of regulated secretion. In contrast, no consistent increase of CSQ discharge was observed with respect to unstimulated preparations incubated in parallel (not shown in figures).

Morphological Studies

The four L6 clones discussed so far for ER protein expression were investigated also by morphological techniques. The results shown refer to C1 and A3, but similar data were obtained also with C2 and H. Fig. 4, *A* and *B*, compares the conventional thin section electron microscopy of undifferentiated cells. Although the general appearance of control and CSQ-infected cells was moderately different, with the latter cells being larger and apparently more flat, the nucleus, mitochondria, ER and Golgi complex (GC) were similar. In addition, however, the CSQ-infected cell (Fig. 4 *B*) showed a series of ovoidal vacuoles, 0.2 to 0.6 μm in the small diameter, often concentrated near the cell surface. Some of these vacuoles appeared filled with a homogeneous, moderately dense content (Fig. 4, *B*, *D*, and *E*); in others the content was more irregular, with a moth-eaten appearance (Fig. 4 *C*). Finally, some of the vacuoles appeared to enclose not one but two to four moderately dense masses, close to each other (not shown). The vacuoles were often located in the proximity of other organelles, particularly ER cisternae and mitochondria, with respect to which, however, they never establish continuous connections, apparently maintaining therefore the status of discrete organelles (Fig. 4 *B*). In the higher magnification insets (Fig. 4, *C–E*) the vacuoles are shown to often possess localized membrane irregularities (duplications, small blebs) which however do not extend into the content.

The molecular composition of the vacuoles was investigated by immunofluorescence and immunogold labeling of undifferentiated L6 cells. Fig. 5 *A* illustrates the delicate immunofluorescent network revealed by the decoration with anti-CR Ab in a control C1 cell. The images obtained with the same Ab in CSQ-infected cells were not appreciably different (not shown). Marked differences between control and infected cells were in contrast revealed when immunofluorescence was addressed to CSQ. In agreement with the Western blot data (Fig. 1), control cells were in fact negative (Fig. 5 *B*) whereas the CSQ-infected cells exhibited a tenuous fluorescence in their background cytoplasm together with numerous, intensely fluorescent puncta visible in over 50% of the cell population. The largest and most prominent puncta were concentrated in the subplasmalemma area, others were spread in the rest of the cell (Fig. 5 *C*). The nature of these CSQ-positive puncta was further investigated by immunogold labeling of ultrathin crio and Epon sections. As can be seen in Fig. 5 (*D* and *G*), the organelles positive for CSQ were vacuoles corresponding in size, shape and distribution to those described by conventional ultrastructural analysis (Fig. 4, compare *B–E*). Interestingly, some of these vacuoles exhibited a multilobular content (Fig. 5 *D*) while others were irregular, enclosing a dense, round, CSQ-positive core in apparent continuity with one or more lighter, largely CSQ-negative structures (Fig. 5 *G*). In addition to the large vacuoles, some degree of CSQ labeling was observed over small, apparently discrete vesicles and within Golgi cisternae, in particular at the periphery and towards the trans Golgi area (Fig. 5, *E* and *F*, and data not shown). Within the ER lumen the CSQ labeling was low and appeared randomly distributed (Fig. 6, *D* and *E*).

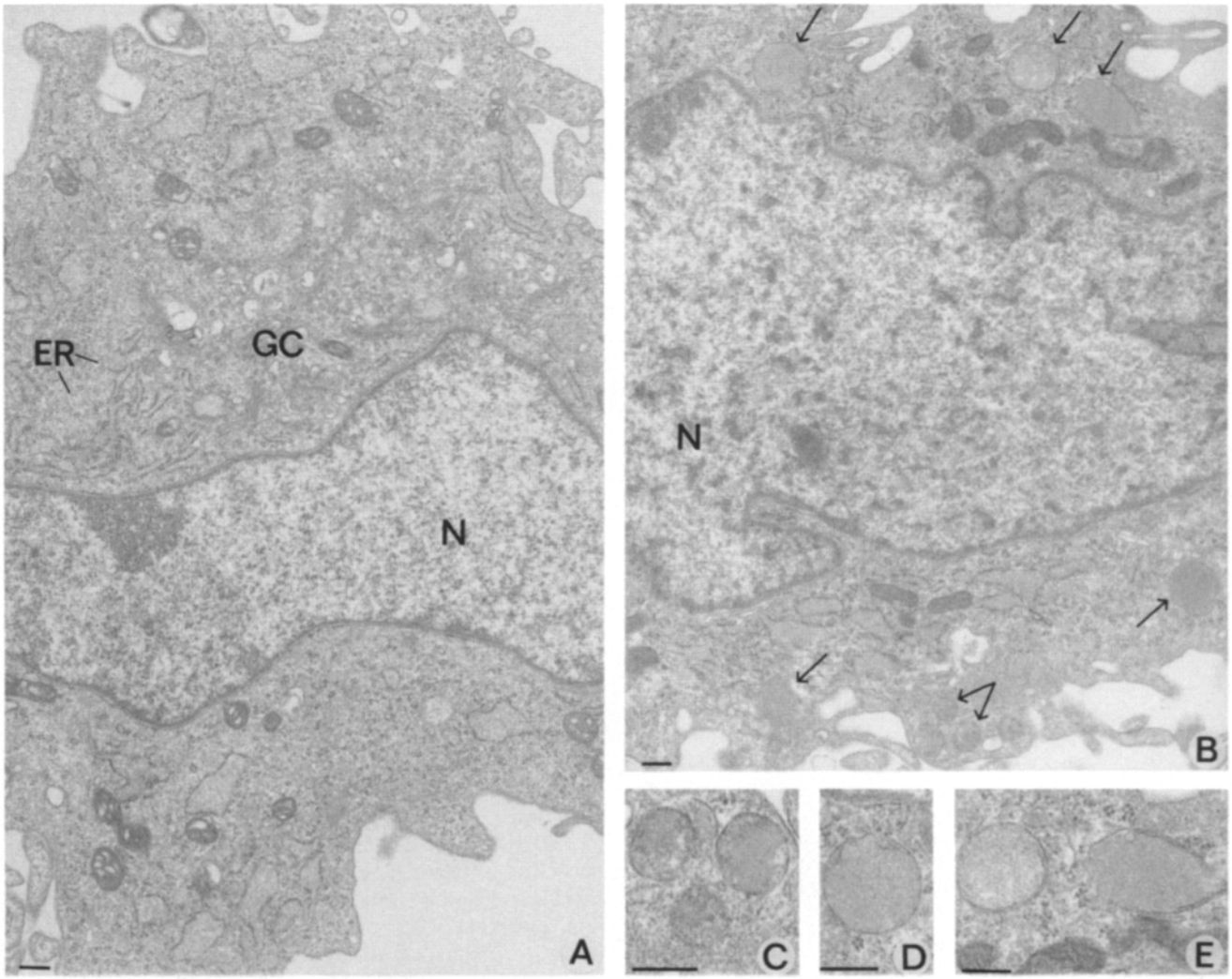

Figure 4. Conventional electron microscopy of undifferentiated control (C1) and CSQ-infected (A3) L6 cells. The control cell (*A*) shows a fibroblast-like phenotype, with numerous, widely distributed rough-surfaced ER cisternae, a well developed Golgi complex (*GC*), dense mitochondria and a flat nucleus (*N*). In the CSQ-infected cell (*B*) all these properties are maintained. In addition the cells show accumulation of large vacuoles of moderate density. At higher enlargement (*C–E*) some of these vacuoles show a homogeneous, others a partially heterogeneous content. The limiting membrane of the vacuoles is locally duplicated or irregular. Bar (in these and in the following electron micrographs) 0.25 μm.

Various possibilities were considered to explain the nature of the CSQ-positive vacuoles revealed in undifferentiated, CSQ-infected L6 cells. Fig. 6 (*A–C*) shows confocal images obtained by the use of 1D3 (Vaux et al., 1990), an Ab addressed to the COOH terminus of the ER lumenal protein, PDI, and recognized also by other ER resident proteins expressing the COOH-terminal tetrapeptide, KDEL. The delicate fluorescent network obtained with this Ab, which closely resembles that of CR (compare Figs. 6, *A* and *B*, with 5 *A*), appeared similar in control and CSQ-infected cells. When, however, the latter cells were doubly labeled for PDI and CSQ, the strong puncta positive for the second protein were seen to correspond to small negative areas in the PDI network (Fig. 6, *B* and *C*). Similar dissociation of the CSQ puncta was observed also with respect to the CR network (not shown). Dual label experiments were carried out also at the ultrathin cryosection immunogold labeling level. Fig. 6 *D* shows that the PDI labeling, concentrated within ER cisternae, was accompanied by only very low labeling for CSQ. The ER localization of PDI is confirmed also in Fig. 6 *E*, where however the major labeled structure is a vacuole that exhibits exclusively CSQ, and not any PDI labeling. Results similar to those of Fig. 6 *E* were obtained in over 40 additional vacuoles.

The results of Fig. 6 exclude the vacuoles of nondifferentiated, CSQ-infected cells to be part of the ER. Fig. 7 (*A* and *B*) explores the possible acidic nature of these organelles, investigated by confocal microscopy of CSQ-infected cells dually labeled for CSQ and DAMP, a weak lipophilic amine accumulated into the acidic compartments (Orci et al., 1986; Hashimoto, 1988). As can be seen, the punctate pattern revealed in the confocal microscope by the Ab against the latter antigen did not appear interrupted in correspondence of most, if not all, CSQ-positive puncta. The possible lysosomal nature of these CSQ-positive acidic organelles was investigated by immunolabeling with anti-cathepsinD (CatD) Abs. At the immunofluorescence level the general distribution of the two antigens, CSQ and CatD,

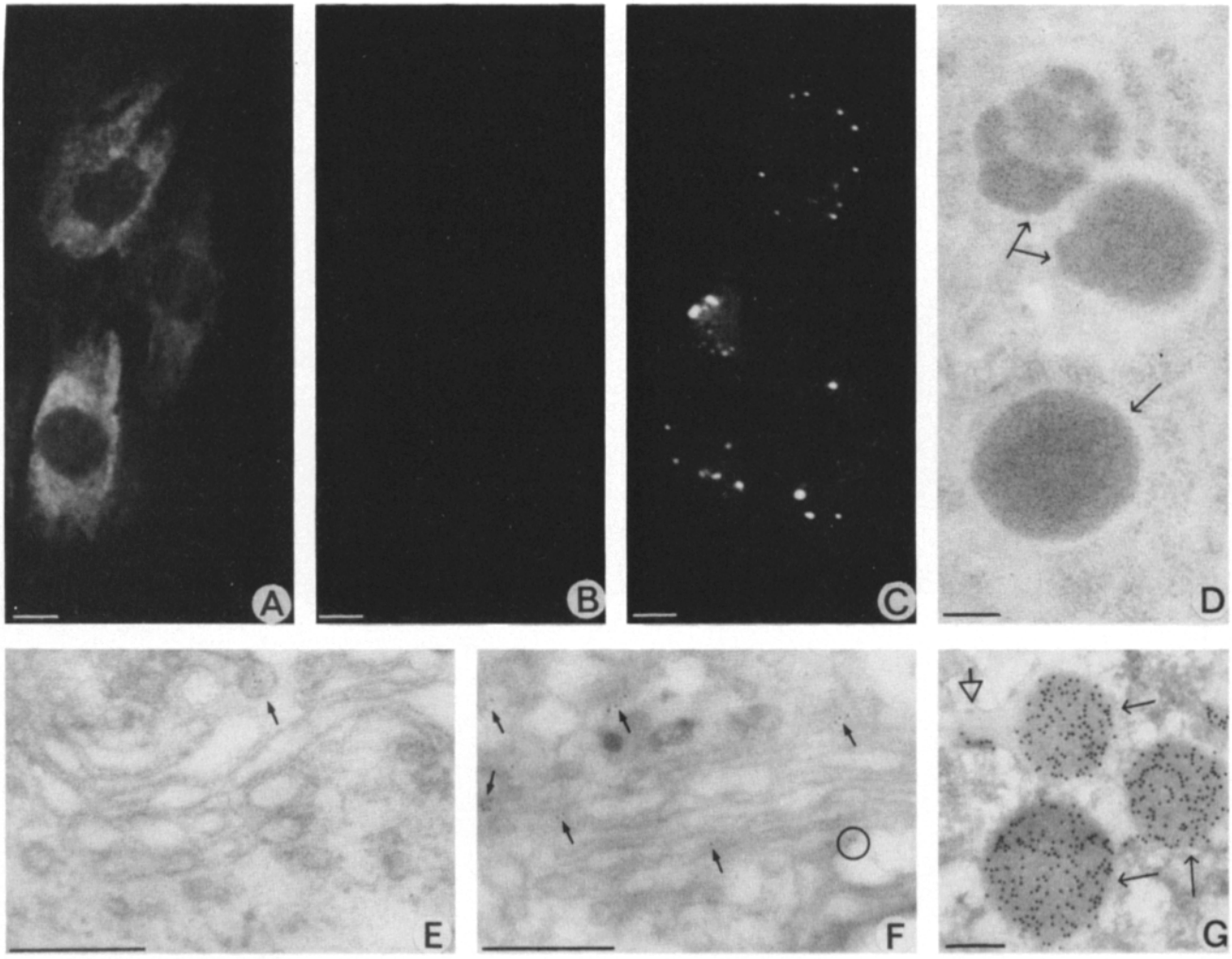

Figure 5. Undifferentiated control (C1) and CSQ-infected (A3) L6 cells. Immunolabeling for CR and CSQ. *A* shows the immunofluorescence labeling for CR and *B* the negative pattern for CSQ in C1 cells. Positivity for CSQ, with intensely fluorescent puncta of various size in a group of CSQ-infected (A3) cells is shown in *C*. *D* and *G* show the intense immunogold labeling of the vacuoles (*thin arrows*) corresponding to the fluorescence puncta, as revealed in a ultrathin Epon section and in a cryosection, respectively. In *G* the open arrow points to a lighter body, with only moderate CSQ labeling, which appears in direct continuity with a typical CSQ-rich vacuole. *E* and *F* show cryosectioned Golgi complex images of infected cells. Weak CSQ labeling is visible over vesicles (*E*) and within Golgi cisternae (*F*). The labeling encircled in *F* might be artifactual. Bar (in *A*, *B*, *C*, and in the following fluorescence micrographs) 10 μm.

appeared similar, except for some large, strongly CSQ-fluorescent puncta near the cell surface (Fig. 7, compare *C* and *E*). Attempts to obtain dually labeled fluorescent preparations yielded however unconvincing results. The problem was therefore reinvestigated at the ultrathin cryosection immunolabeling level. As can be seen in Fig. 7 (*F* and *H–K*) colabeling for the two antigens was observed in a large population of vacuoles which however appeared not homogeneous but distributed in two populations. Those with a denser content were most often rich in CSQ and showed low CatD immunolabeling (Fig. 7, *F*, *H*, and *I*). Other vacuoles, of lighter content, exhibited a variable CatD positivity and a low CSQ signal which, considering the relatively high background of the large gold immunolabeling, was often at or just above the specificity levels (Fig. 7, *F* and *K*). In some cases, vacuoles of the two types were closely adjacent, suggesting a membrane continuity (Fig. 7 *F*) similar to that already mentioned in Fig. 5 *G*. A plot summarizing the CSQ/CatD immunolabeling properties of the investigated vacuoles is shown in Fig. 7 *G*.

Morphological studies were carried out also on L6 cells after differentiation induced by serum starvation. Fig. 8 (*A* and *B*) shows conventional images of control C1 cell ultrastructure, documenting 7 d changes with respect to growing cells, including large prevalence of the myotube phenotype and appearance of muscle markers, such as the myofibrillae, with marked development of the smooth ER. Similar changes were observed in the other control clone, C2, and in the two CSQ-infected clones, A3 and H (not shown). At the immunofluorescence level the positivity for CSQ appeared now distributed throughout the cytoplasm, more prominent in the clones infected for the Ca^{2+}-binding protein than in the controls. Intensely fluorescent puncta were still evident, expressed however not by the majority but by <5% of the infected cells (Fig. 8 *D*). In the analyzed population the number of puncta/cell was 0.07, i.e., 1.7% with re-

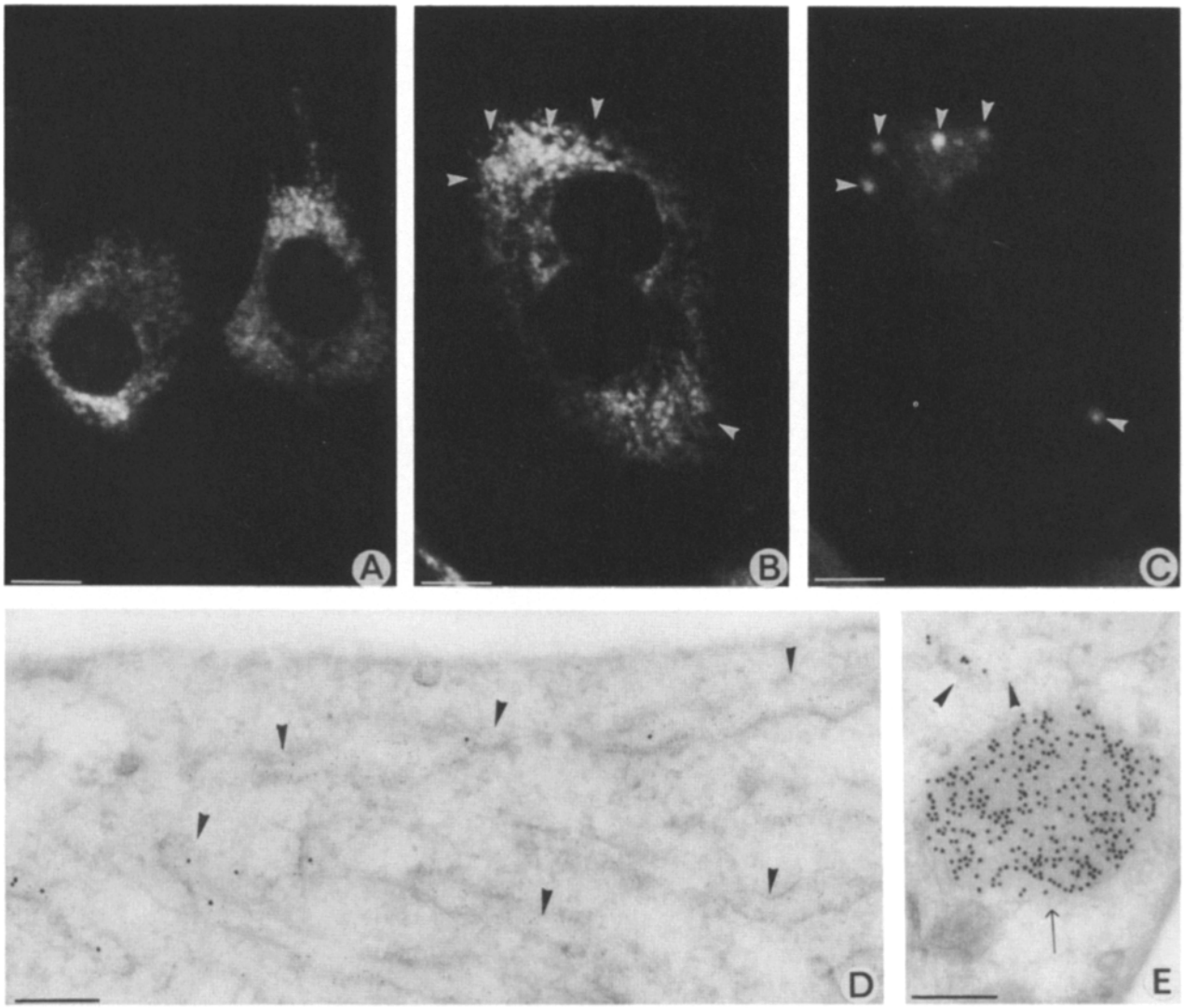

Figure 6. Immunolabeling for PDI and CSQ in undifferentiated L6 cells. *A* shows the PDI fluorescence labeling of a control C1 cell, and *B* and *C* dual labeling for PDI and CSQ in an infected cell (A3). In both panels the white arrowheads point to the CSQ puncta and the corresponding holes in the PDI pattern. *D* and *E* show dual, PDI (small gold)/CSQ (large gold) immunolabeled ultrathin cryosections. Notice, the almost uniform distribution of PDI throughout the ER lumen (*arrowheads*), with few accompanying CSQ-labeling gold particles; and the intense CSQ labeling of a vacuole which is completely PDI negative (*thin arrow*, *E*).

spect to the corresponding value in undifferentiated cells. Interestingly, the CSQ-positive puncta were visible not only in the infected cells but appeared also in a fraction (~2%) of the controls (Fig. 8 *C*). At later stages of differentiation (10 and 20 d) the puncta were visible neither in the infected nor in the control cells. In these more differentiated populations a fraction of the cells were of higher volume, with larger accumulation of CSQ.

Immunogold labeling of the 7-d cells revealed that the few CSQ-rich vacuoles (not shown) were undistinguishable from those of the growing cells. Profoundly different was in contrast the CSQ labeling of the ER lumen (Fig. 8, *E* and *F*). On the one hand, it was much more intense than in undifferentiated cells; on the other hand, it was not evenly distributed but concentrated into discrete areas whereas other areas, in particular long cisternae, remained negative. Comparison of infected and control cells confirmed a moderately higher labeling in the first (Fig. 8, compare *E* and *F*), which however was not quantitated morphometrically.

$[Ca^{2+}]_i$ Responses

These experiments, carried out in suspensions of fura-2–loaded cells, were aimed at investigating whether expression of CSQ in the infected cells was inducing changes of intracellular Ca^{2+} homeostasis. Fig. 9 shows the concentration dependence of the $[Ca^{2+}]_i$ peak responses induced by the administration (in the Ca^{2+}-free medium) of vasopressin (Vp), a peptide hormone that in L6 cells is addressed to the V_1 receptor. The latter is a receptor coupled to the hydrolysis of polyphosphoinositides, which induces generation of IP_3 and thus release of Ca^{2+} from the stores. As can be seen, in the undifferentiated cells (Fig. 9 *A*) the $[Ca^{2+}]_i$ responses induced by the whole range of peptide concentra-

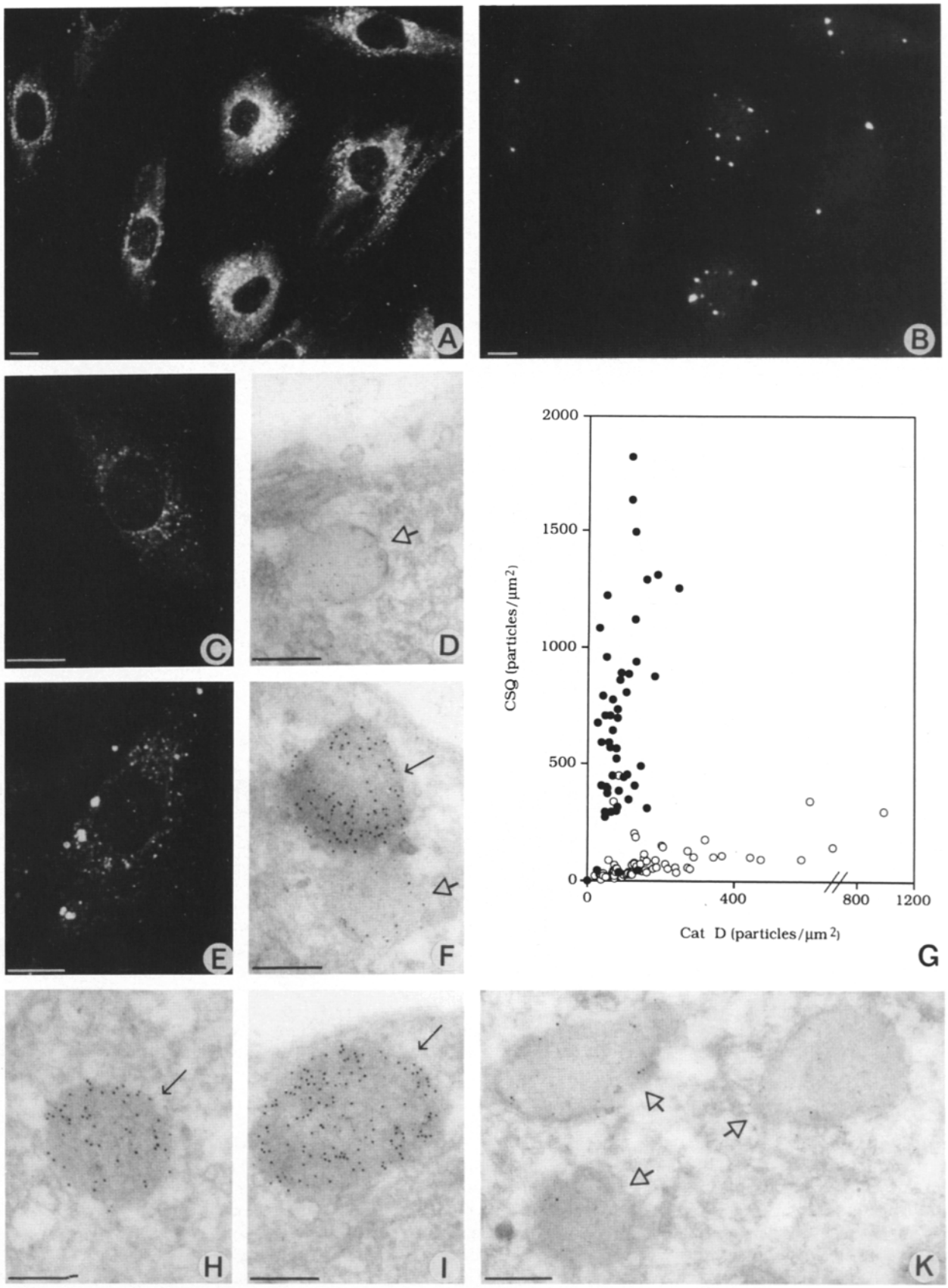

Figure 7. Immunolabeling for DAMP, CatD, and CSQ of undifferentiated, CSQ-infected (A3) L6 cells. *A* and *B* show a dual immunofluorescence labeling for DAMP and CSQ in a group of infected cells. Notice that the brightly fluorescent puncta positive for the latter protein seem not to interrupt the granular pattern revealed in the cells for the weak amine. *C* and *E* show two different cells fluorescently labeled one for CatD, the other for the Ca^{2+}-binding protein. Double label for CatD (small gold) and CSQ (large gold), is shown in the ultrathin cryosections of *D*, *F*, and *H–K*. Notice that in the vacuoles the higher density of the content is accompanied by stronger CSQ positivity (*F*, *H*, and *I*, *thin arrows*) whereas the lighter content is poor of CSQ and more labeled for CatD (*D*, *F*, and *K*, *open arrows*). In *F* one dense and one light vacuoles are close to each other, suggesting membrane continuity. *G* shows in a plot the quantitation of the CSQ/CatD labeling data. Closed circles are the dense, and open circles the light vacuoles analyzed.

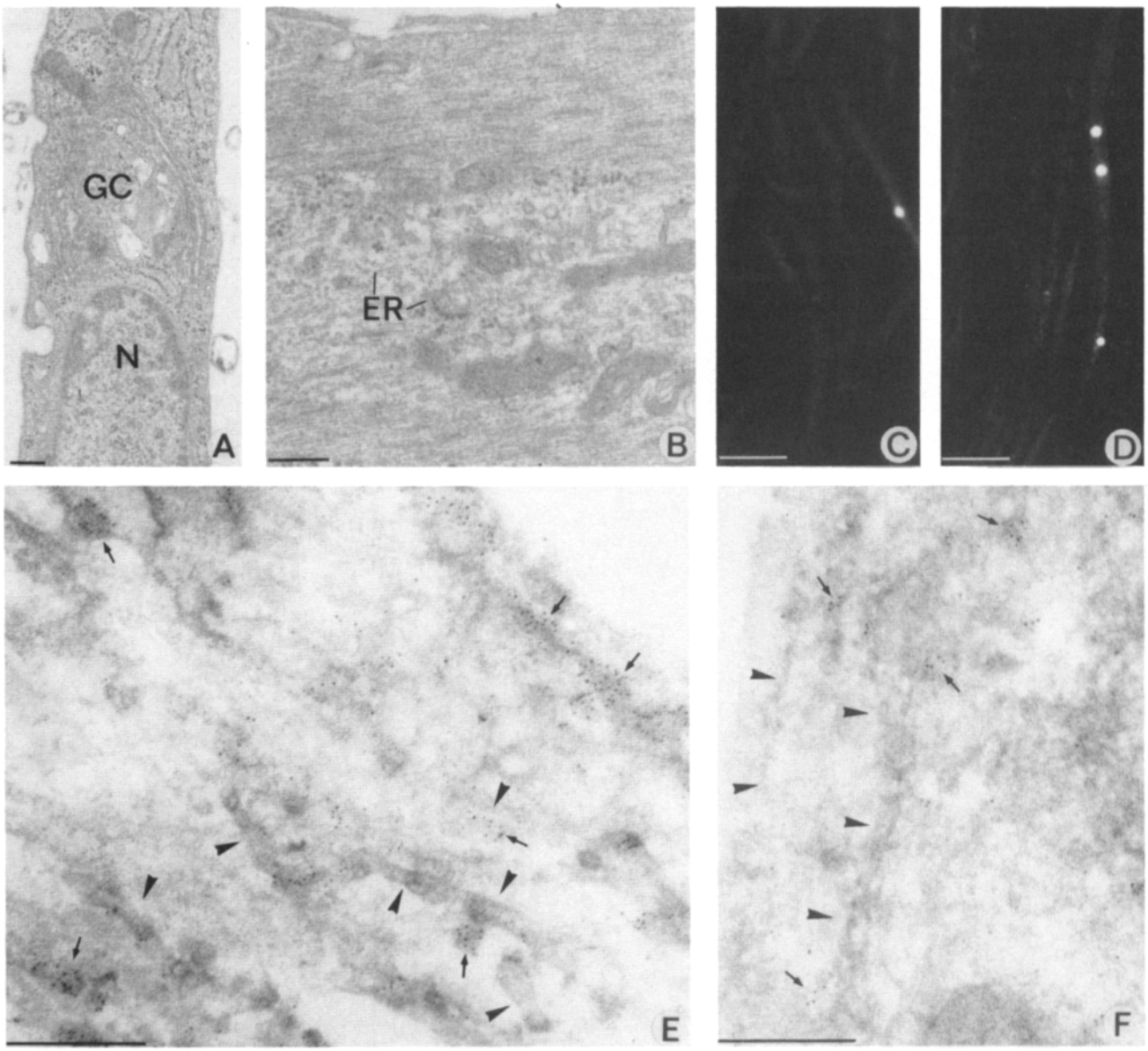

Figure 8. Differentiated control (C1) and CSQ-infected (A3) L6 cells, shown in conventional electron microscopy, immunofluorescence, and ultrathin cryosection immunogold labeling for CSQ. *A* and *B* illustrate the conventional electron microscopy of control cells that show clear signs of differentiation, with a myotube phenotype, accumulation of myofibrils and development of the ER. *C* and *D* show the CSQ immunofluorescence images of controls and infected cells, respectively, chosen because of the occurrence of a few intensely fluorescent vacuoles in a cell minority of both preparations. The distribution of the labeling appeared primarily into a delicate network, more evident in the CSQ-infected cells. In the ultrathin cryosections (*E* and *F*, infected and control cell, respectively) such a network appears to be composed by ER cisternae which however appear partially filled with (*small arrows*) and partially devoid of (*arrowheads*) the immunogold-labeled antigen.

tions remained essentially the same in the four clones investigated, no matter whether control or CSQ infected, in spite of the expression in the latter cells of considerable amounts of the Ca^{2+}-binding protein. Fig. 9 *B* shows the corresponding peak responses observed in two clones, C1 and A3, investigated after 7 d differentiation treatment. As can be seen, the responses of the CSQ-infected clone were now larger than in the control, not so much however at low and maximal but rather at intermediate Vp concentrations, especially at 10 nM where the difference observed was about 2:1 in 12 experiments.

The results of Fig. 10 extend the study of Ca^{2+} homeostasis from the IP_3 sensitive, rapidly exchanging stores to the other Ca^{2+} stores of undifferentiated and differentiated L6 cells, controls and CSQ infected. The rationale of the experiments lies on the administration to the cell suspensions (in Ca^{2+}-free medium) first of the optimal concentration of Vp (10 nM, Fig. 9) followed in sequence, after the exhaustion of the preceding response, by maximal concentrations of the SERCA pump blocker, Tg; of the Ca^{2+} ionophore, ionomycin; and finally of the H^+/Na^+ ionophore, monensin. Under the conditions of the experiment Tg is expected to release the

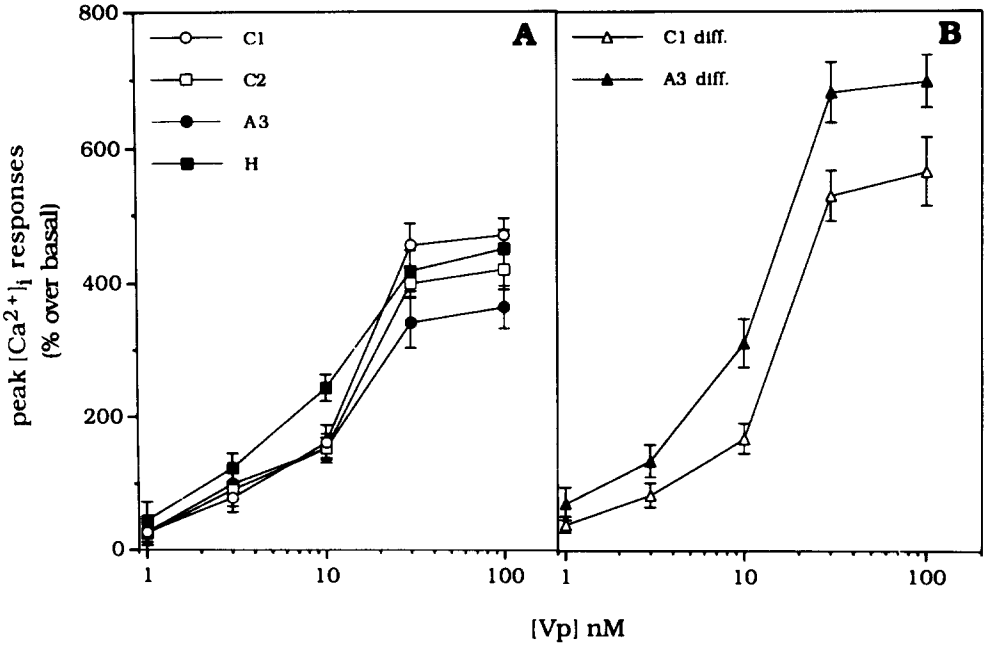

Figure 9. $[Ca^{2+}]_i$ peak increase responses induced by increasing concentrations of Vp in the various L6 clone cells suspended in the Ca^{2+}-free medium. *A* illustrates the responses of the control (C1 and C2) and CSQ-infected (A3 and H) clones analyzed while undifferentiated; *B* of the C1 and A3 clones analyzed after 7-d differentiation. Values shown are averages ± SD.

part of the ER Ca^{2+} pool remaining after the Vp treatment, due however to unopposed leakage from the store rather than to activation of a channel; ionomycin is expected to release Ca^{2+} pools from non ER stores with non-acidic lumen; and monensin (working in association with ionomycin), the pools from acidic stores (Fasolato et al., 1991). Fig. 10 (*A* and *C*) concerns the C1 clone; (*B* and *D*) the A3 clone. As can be seen, differentiation of the control cells fails to modify not only the $[Ca^{2+}]_i$ responses induced by Vp, but also those by the other treatments. In the CSQ-infected cells, on the other hand, the increased response to 10 nM Vp observed after differentiation was not accompanied by any changes in response to the other treatments administered (Fig. 10, *B* and *D*).

Discussion

In the present work we have investigated the expression of heterologous CSQ, the major Ca^{2+}-binding protein of muscle SR, in stable clones of a myoblast cell line that does express CSQ homologously together with other skeletal muscle markers, however only after differentiation. Some concern about our approach could come from the fact that the protein and cells used were from different animal species, chicken and rat, respectively. In the chicken, only one form of CSQ is known, localized in both heart and muscles, whereas in mammals two forms are expressed, one in fast-twitch muscles, the other in the heart, while in the slow-twitch and in the smooth muscles these two forms coexist within individual fibers (see Pozzan et al., 1994; Volpe et al., 1994). Although the general structure of the chicken CSQ is very similar to that of the mammalian proteins, a few of its amino acid sequences are peculiar (compare Clegg et al., 1988 with Fliegel et al., 1987, and Scott et al., 1988) and its glycosylation pattern is not yet known. The possibility should thus be considered that the accumulation of the chicken CSQ we have observed within the large vacuoles of infected, non differentiated L6 cells represents the result not of physiological sorting, but of some type of unspecific "rejection" process of the heterologous protein. Based on the available evidence, however, this possibility appears highly unlikely. In fact: (*a*) CSQ-rich vacuoles, such as those described here in L6 cells, were seen to develop in other types of mammalian cells as well (human epithelial HeLa and mouse C_2 myoblasts) when infected with the cDNA not only of the chicken but also of a mammalian (rabbit) CSQ (Villa, A., J. Meldolesi, and P. Volpe, unpublished observations); (*b*) CSQ-rich vacuoles appeared not only in undifferentiated, infected cells, but also in a small fraction of controls at an early stage of differentiation, i.e., when these cells begin to synthesize the endogenous rat CSQ (see Figs. 3 and 8); and (*c*) in fully differentiated L6 cells, no matter whether control or CSQ infected, the Ca^{2+}-binding protein was no longer sorted to the vacuoles, but entirely retained within its site of physiological localization, the ER. This last result demonstrates the "compatibility" of the chicken CSQ (which in the differentiated infected cells accounts for >50% of the total) for the sorting mechanisms of rat L6 cells. We conclude therefore that the differential distribution of the heterologous CSQ observed in L6 cells depends on their state of differentiation. Moreover, the $[Ca^{2+}]_i$ results obtained in the infected cell populations before and after differentiation demonstrate that such a differential distribution of CSQ has profound effects on the responses triggered by a IP_3 generating treatment.

In the skeletal, cardiac and smooth muscle fibers, as well as in avian Purkinje neurons, i.e., the cell types where CSQ is physiologically expressed, synthesis on the membrane-bound polysomes (by the signal sequence–SRP mechanism) is known to be followed by the lumenal concentration of the protein within specialized areas of the ER (SR terminal and corbular cisternae; calciosomes; see Pozzan et al., 1994). Such a localization cannot be due to the recycling from the GC, which has been demonstrated for other ER lumenal proteins, since CSQ misses the COOH-terminal sequence address, KDEL (Fliegel et al., 1987; Scott et al., 1988; Clegg

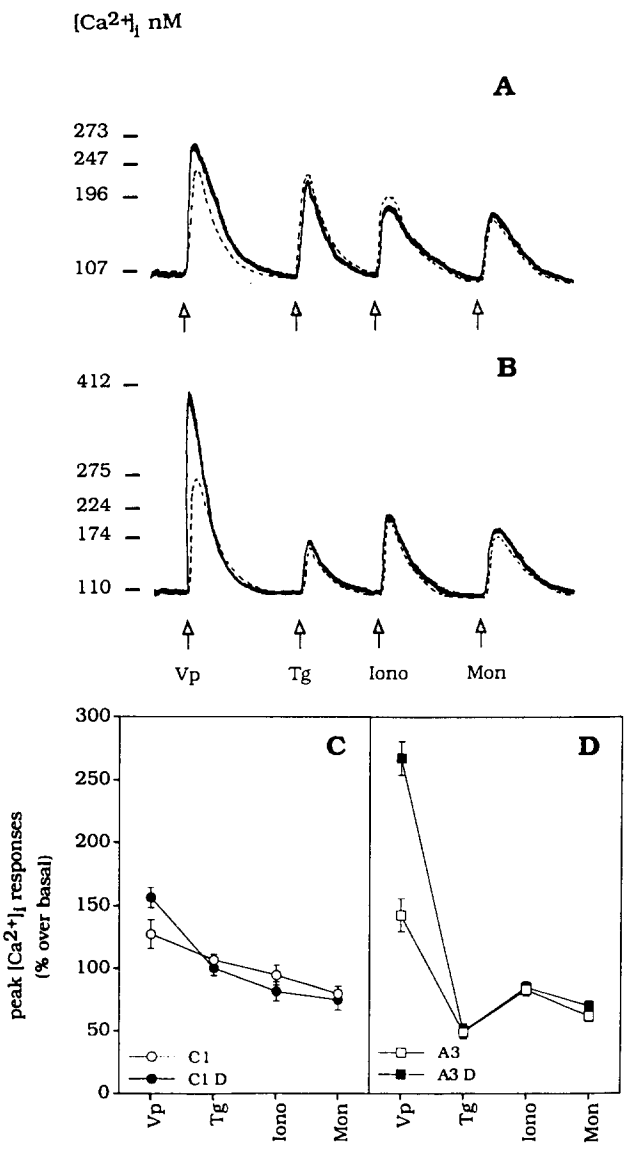

Figure 10. Comparison of the $[Ca^{2+}]_i$ responses induced by the subsequent, additive administration of Vp, Tg, ionomycin, and monensin to control (Cl) and CSQ-infected (A3) clone cells analyzed, while suspended in Ca^{2+}-free medium, before and after 7-d differentiation. *A* shows typical responses of Cl cells and *B* those of A3 cells. (*Broken lines*) undifferentiated; (*continuous lines*) differentiated cells. The drugs (*arrows*) were administered at the following concentrations: *Vp*, 10 nM; *Tg*, 0.1 μM; ionomycin (*Iono*), 0.5 μM; monensin (*Mon*), 1 μM. *C* and *D* show the corresponding average peak values ± SD obtained in six separate experiments. *Cl* and *A3*, and *ClD* and *A3D* refer to the two clones, undifferentiated and 7-d differentiated, respectively.

et al., 1988). Rather, CSQ masses appear to assemble and might be directly attached to membrane protein(s) protruding into the lumen (Franzini-Armstrong et al., 1987). Various proteins have been proposed to play this CSQ anchoring role (Mitchell et al., 1988; Damiani and Margreth, 1990; Knudson et al., 1993). None, however, has been identified with certainty yet.

In the growing, undifferentiated L6 cells only a tiny fraction of the heterologous CSQ was revealed within the ER, apparently intermixed at random with other lumenal proteins, the bulk being concentrated within the vacuoles. At variance with previously described bodies of different specificity (Sitia and Meldolesi, 1992), these last organelles cannot be part of the ER because of their negativity for abundant ER lumenal proteins, such as PDI and CR. These results strongly suggest that growing L6 cells are devoid of the mechanisms to keep CSQ in its ER location. As a consequence, the Ca^{2+}-binding protein appears to be transported along the exocytic pathway, ending up into the vacuoles.

Information about the assembly of the latter structures may be deduced from our ultrastructural and immunocytochemical findings. Within the GC of growing infected cells the CSQ labeling was found to be weak, revealing no major concentration with respect to the ER. The observation of small foci of labeling within individual cisternae, particularly towards the trans side, suggests however that CSQ-containing vesicles might pinch off from the GC. The rarity of discrete CSQ-labeled vesicles in the surrounding cytoplasm, together with the observation of vacuoles exhibiting a multilobated content, suggest the GC-derived vesicles to be destined to rapid fusion, and CSQ concentration to occur primarily within the large vacuoles. Because of these probable processes, the newly assembled CSQ-rich vacuoles may appear akin to prelysosomes or even to secretion granules, a nature that might explain also the acidity of their content revealed by the labeling with DAMP. In addition, appreciable amounts of the heterologous CSQ were recovered in the incubation medium. Since, however, release of CSQ did not increase when the cells were exposed to ionomycin, an ionophore that stimulates regulated secretion from a variety of secretory cells, the involvement of regulated secretion granules appears unlikely.

Most CSQ-rich vacuoles were positive not only for the acidity marker, DAMP, but also for the lysosomal enzyme, CatD. How could the vacuoles pick up their modest, but appreciable, levels of this and, presumably, other lysosomal enzymes? The fact that the vacuoles do not coincide with the whole lysosome population, but with a subpopulation, makes unlikely the involvement of the molecular transport mechanisms specific for mannose-6-phosphate and its receptors. Alternatively, at least three processes have been described for the lysosomal conversion of intracellular structures: autophagocytosis (see Dunn, 1990*a*, *b*), ER–lysosomal diversion (Noda and Farquhar, 1992) and crinophagy (Smith and Farquhar, 1966; Farquhar, 1969). In our cells, autophagocytosis and diversion appear unlikely, the first because the vacuole content did exhibit neither recognizable organelles nor myelin figures, as expected from the unspecific engulfment of volumes of the cytoplasm; the second because intermediate stages of ER processing, preceding the appearance of lysosomal enzyme positivity, were never observed. Moreover, as already mentioned, the vacuoles were negative for ER lumenal proteins, PDI and CR. At the present time, therefore, the most likely explanation appears crinophagy, i.e., the direct fusion of lysosomes with the vacuoles. This interpretation appears supported by images suggesting vacuole–lysosome fusion and by the irregularities of the limiting membrane, observed in the vacuoles by conventional electron microscopy, which could result from the fusion process. Moreover, crinophagy could explain the observation that only the authentic and not the

faster CSQ isoform is released to the medium, if we assume that after lysosome fusion (the process that presumably leads by proteolysis to the generation of the faster band) the vacuoles loose their property to be discharged at the plasmalemma. Whatever the biogenetic process, what is clear is that the CSQ-rich vacuoles account for only a fraction of the cell lysosomes, while the others contain no or only small concentrations of CSQ.

The $[Ca^{2+}]_i$ study of the undifferentiated, CSQ-infected L6 cells provided additional information about the vacuoles. The lack of major differences in the responses to Vp with respect to the controls was expected. The hormone action on $[Ca^{2+}]_i$ occurs in fact via the generation of IP_3 and the release of Ca^{2+} from stores located in the ER, an organelle that CSQ infection left substantially unchanged in the undifferentiated cells (only minimal levels of CSQ within the lumen; no change of other components, including CR and the IP_3 receptor). Unexpected, in contrast, were the results obtained with ionophores, ionomycin and monensin. In particular, the combination of these two drugs is known to induce discharge of Ca^{2+} from organelles with acidic lumena (Fasolato et al., 1991), such as the vacuoles. CSQ is a high capacity protein that maintains large part of its Ca^{2+}-binding activity in an acidic environment (Mac Lennan and Wong, 1971). Since its concentration within the vacuoles is high, an increased Ca^{2+} release after the combined treatment with the two ionophores was to be expected. The only explanation for the negative result is that vacuoles contain no accumulated Ca^{2+}, presumably because their membrane contains no Ca^{2+} ATPase.

Differentiation of L6 cells yielded profound transformations of their structural and functional properties. Already at 7 d a switch occurred in control cells between the major ER lumenal Ca^{2+}-binding proteins, with decrease of CR and appearance of the homologous CSQ. Since these two events occurred concomitantly, they probably tended to compensate for each other, thus explaining why no major changes occurred in the Vp-induced $[Ca^{2+}]_i$ responses of control cells. The same changes of endogenous CR and CSQ occurred also in the infected cells which however, in spite of their marked decrease of the heterologous CSQ, nevertheless exhibited $[Ca^{2+}]_i$ responses to Vp considerably larger than those in both controls and non-differentiated, CSQ-infected cells. Such an increase of the Vp responses appears to correlate well with the change of the CSQ distribution. In the differentiated cells, in fact, the CSQ immunolabeling was restricted almost exclusively to the ER lumen. Thus, although no Abs are available to us that discriminate between homologous and heterologous CSQs, we can nevertheless conclude that these two forms were co-accumulated at that site, in clear excess with respect to the decrease of CR. This excess is most likely responsible for the increased Ca^{2+} capacity of the IP_3-sensitive stores, revealed by the release experiments with Vp. Moreover, in the infected differentiated (and also in the control) cells the immunogold labeling of the ER was clearly non-random, with concentration in specific areas and apparently complete lack in others. Retention and non-random distribution of CSQ within the ER can only be attributed to the appearance during differentiation of the so far unidentified mechanisms for the development and anchorage of the CSQ masses discussed above in the other cells that express the protein.

In the differentiated L6 cells the CSQ masses might occur in the proximity of IP_3 receptor clusters, as it is the case for the smooth muscle SR (Villa et al., 1993*a*) and also for the striated muscle SR with the ryanodine receptors (Franzini-Armstrong et al., 1987). This could explain why higher differences in $[Ca^{2+}]_i$ responses between controls and infected cells were better observed at submaximal rather than at maximal concentrations of Vp. With strong stimulations, because of the general recruitment of IP_3 receptors, the Ca^{2+} release could in fact come not only from the specialized, but also from the remaining areas of the ER, which appear to participate little in CSQ accumulation.

In conclusion, the results that we have reported have permitted us to trace the distribution of CSQ, the major muscle SR Ca^{2+}-binding protein, when expressed in a myoblast line before and after differentiation. Expression of the protein by the undifferentiated L6 cells, which are not equipped for this task, has revealed accumulation within a post-GC vacuolar compartment which appears to largely correspond to a lysosomal subpopulation and which, although much less prominent, does develop also in a fraction of the control cells once the synthesis of the homologous CSQ is initiated during differentiation. The CSQ-rich vacuoles seem to be poor of Ca^{2+} within their lumen, a property that, to our knowledge, had never been reported for any cytoplasmic organelles (see Pozzan et al., 1994). It was only in the infected differentiated L6 cells, where accumulation of CSQ occurs not much within the vacuoles but within the compartment of physiological localization, the ER, that a functional correlate of the Ca^{2+}-binding protein expression was revealed, i.e., an increase of the IP_3-mediated Ca^{2+} release. These observations document two phenomena which, although widely accepted, were supported up until now by little if any experimental evidence in intact myoblastic cells: the development during differentiation of specific mechanism(s) of CSQ retention in the ER; and the direct contribution of CSQ, when appropriately retained in the ER, to the Ca^{2+} capacity of the IP_3-sensitive, rapidly exchanging Ca^{2+} stores. The availability of the infected L6 cell model we have described, where expression of CSQ and its retention in the ER can be dissociated, is expected to ultimately prove useful for the identification of the retention mechanism(s) that so far have remained elusive when investigated in the cells of physiological expression, such as the various types of muscle fibers.

The technical assistance of G. Racchetti and M. Bossi and the typing assistance of L. Di Giorgio are gratefully acknowledged. We also thank Dr. P. Podini for participating in the morphological work, and Drs. F. Valtorta, A. Malgaroli, and R. Fesce for critically reading the paper. The purified chicken and rabbit CSQ, and the rat liver CR were the generous gifts of Dr. P. Volpe (University of Padova, Padova, Italy). The antibodies against IP_3 receptor, SERCA, CR, PDI (C terminal sequence, 1D3, and the bovine enzyme), CatD, and ER membrane proteins were the kind gifts of Drs. A. H. Sharp (Johns Hopkins University, Baltimore, MD); M. East (University of Southampton, Southampton, U.K.); H. D. Söling (University of Göttingen, Göttingen, Germany); S. Fuller (EMBL, Heidelberg, Germany); F. Baccino (University of Torino, Torino, Italy) and D. Louvard (Pasteur Institute of Paris, Paris, France), respectively. We thank Mr. C. Albrile and the Zeiss Italy for the use of the LSM confocal scanning microscope, and W. Pabisch of Milano for the use of the cryo-ultramicrotome.

M. Raichman was supported by a San Raffaele fellowship and P. Papazafiri by a European Community fellowship. Partial support for this work was provided by grants from CNR (Target Project Biotechnology) and the European Community (Copernicus Program, CIPA-CT 92-3014).

Received for publication 13 June 1994 and in revised form 15 September 1994.

References

Bender, M. A., T. D. Palmer, R. E. Gelinas, and A. D. Miller. 1987. Evidence that the packaging signal of Moloney murine leukemia virus extends into the gag region. *J. Virol.* 61:1639–1646.

Berridge, M. J. 1993. Inositol trisphosphate and calcium signalling. *Nature (Lond.).* 361:315–325.

Choi, E. S. H., and D. O. Clegg. 1991. Identification and developmental expression of a chicken calsequestrin homologue. *Dev. Biol.* 142:169–177.

Clegg, D. O., J. C. Helder, B. C. Hann, D. E. Hall, and L. F. Reichardt. 1988. Amino acid sequence and distribution of mRNA encoding a major skeletal muscle laminin-binding protein: an extracellular matrix-associated protein with an unusual COOH-terminal polyaspartate domain. *J. Cell Biol.* 107:699–705.

Colyer, J., A. M. Mata, A. G. Lee, and J. M. East. 1989. Effects on ATPase activity of monoclonal antibodies raised against ($Ca^{2+}Mg^{2+}$)-ATPase from rabbit skeletal muscle sarcoplasmic reticulum and their correlation with epitope location. *Biochem. J.* 262:439–446.

Damiani, E., and A. Margreth. 1990. Specific protein-protein interactions of calsequestrin with junctional sarcoplasmic reticulum of skeletal muscle. *Biochem. Biophys. Res. Commun.* 172:1253–1259.

Dunn, W. A. 1990*a*. Studies on the mechanisms of autophagy: formation of the autophagic vacuole. *J. Cell Biol.* 110:1923–1933.

Dunn, W. A. 1990*b*. Studies on the mechanisms of autophagy: maturation of the autophagic vacuole. *J. Cell Biol.* 110:1935–1945.

Farquhar, M. G. 1969. Lysosome function in regulating secretion: disposal of secretory granules in cells of the anterior pituitary gland. *In* Lysosomes in Biology and Pathology. J. T. Dingle and H. B. Fell, editors. North-Holland, Amsterdam. 462–482.

Fasolato, C., M. Zottini, E. Clementi, D. Zacchetti, J. Meldolesi, and T. Pozzan. 1991. Intracellular Ca^{2+} pools in PC12 cells. Three intracellular pools are distinguished by their turnover and mechanisms of Ca^{2+} accumulation, storage, and release. *J. Biol. Chem.* 266:20159–20167.

Fliegel, L., M. Ohnishi, M. R. Carpenter, V. K. Khanna, R. A. F. Reithmeier, and D. H. MacLennan. 1987. Amino acid sequence of rabbit fast-twitch skeletal muscle calsequestrin deduced from cDNA and peptide sequencing. *Proc. Natl. Acad. Sci. USA.* 84:1167–1171.

Flucher, B. E. 1992. Structural analysis of muscle development: transverse tubules, sarcoplasmic reticulum, and the triad. *Dev. Biol.* 154:245–260.

Franzini-Armstrong, C., L. J. Kenney, and E. Varriano-Marston. 1987. The structure of calsequestrin in triads of vertebrate skeletal muscle: a deep-etch study. *J. Cell Biol.* 105:49–56.

Grynkiewicz, G., M. Poenie, and R. Y. Tsien. 1985. A new generation of Ca^{2+} indicators with greatly improved fluorescent properties. *J. Biol. Chem.* 260:3440–3450.

Hall, D. E., K. A. Frazer, B. C. Hann, and L. F. Reichardt. 1988. Isolation and characterization of a laminin binding protein from rat and chick muscle. *J. Cell Biol.* 107:687–697.

Hashimoto, S., B. Bruno, D. P. Lew, T. Pozzan, P. Volpe, and J. Meldolesi. 1988. Immunocytochemistry of calciosomes in liver and pancreas. *J. Cell Biol.* 107:2523–2531.

Keller, G. A., T. Tokuyasu, A. H. Dutton, and S. J. Singer. 1984. An improved procedure for immunoelectron microscopy: ultrathin plastic embedding of immunolabeled ultrathin frozen sections. *Proc. Natl. Acad. Sci. USA.* 81:5744–5747.

Knudson, C. M., K. K. Stang, C. R. Moomaw, C. A. Slaughter, and K. P. Campbell. 1993. Primary structure and topological analysis of a skeletal muscle-specific junctional sarcoplasmic reticulum glycoprotein (triadin). *J. Biol. Chem.* 268:12646–12654.

Louvard, D., H. Reggio, and G. Warren. 1982. Antibodies to the Golgi complex and rough endoplasmic reticulum. *J. Cell Biol.* 92:92–107.

MacLennan, D. H., and P. T. S. Wong. 1971. Isolation of a calcium-sequestering protein from sarcoplasmic reticulum. *Proc. Natl. Acad. Sci. USA.* 68: 1231–1235.

Michalak, M., R. E. Milner, K. Burns, and M. Opas. 1992. Calreticulin. *Biochem. J.* 285:681–692.

Mitchell, R. D., H. K. B. Simmerman, and L. R. Jones. 1988. Calcium binding effects on protein conformation and protein interactions of canine cardiac calsequestrin. *J. Biol. Chem.* 263:1376–1381.

Muller, S. R., P. D. Sullivan, D. O. Clegg, and S. C. Feinstein. 1990. Efficient infection and expression of heterologous genes in PC12 cells. *DNA Cell Biol.* 9:221–229.

Noda, T., and M. G. Farquhar. 1992. A non-autophagic pathway for diversion of ER secretory proteins to lysosomes. *J. Cell Biol.* 119:85–97.

Opas, M., E. Dziak, L. Fliegel, and M. Michalak. 1991. Regulation of expression and intracellular distribution of calreticulin, a major calcium binding protein of nonmuscle cells. *J. Cell. Physiol.* 149:160–171.

Orci, L., M. Ravazzola, M. Amherdt, O. Madsen, A. Perrelet, J. D. Vassali, and R. G. W. Anderson. 1986. Conversion of proinsulin to insulin occurs coordinately with acidification of maturing secretory vesicles. *J. Cell Biol.* 103:2273–2281.

Pelham, H. R. B. 1988. Evidence that luminal ER proteins are sorted from secreted proteins in a post-ER compartment. *EMBO (Eur. Mol. Biol. Organ.) J.* 7:913–918.

Peng, Y.-W., A. H. Sharp, S. H. Snyder, and K.-W. Yau. 1991. Localization of the inositol 1,4,5-trisphosphate receptor in synaptic terminals in the vertebrate retina. *Neuron.* 6:525–531.

Perrin, D., B. Sonnichsen, H. D. Soling, and P. Nguyen-Van. 1991. Purkinje cells of rat and chicken cerebellum contain calreticulin (CaBP3). *FEBS (Fed. Eur. Mol. Biol. Organ.) Lett.* 294:47–51.

Pozzan, T., R. Rizzuto, P. Volpe, and J. Meldolesi. 1994. Molecular and cellular physiology of intracellular Ca^{2+} stores. *Physiol. Rev.* 74:595–637.

Sambrook, J., E. F. Fritsch, and T. Maniatis. 1989. Molecular Cloning: A Laboratory Manual. Cold Spring Harbor Press, Cold Spring Horbor, NY.

Scott, B. T., H. K. B. Simmerman, J. H. Collins, B. Nadal-Ginard, and L. R. Jones. 1988. Complete amino acid sequence of canine cardiac calsequestrin deduced by cDNA cloning. *J. Biol. Chem.* 263:8958–8964.

Sitia, R., and J. Meldolesi. 1992. Endoplasmic reticulum: a dynamic patchwork of specialized subregions. *Mol. Biol. Cell.* 3:1067–1072.

Smith, R. E., and M. G. Farquhar. 1966. Lysosome function in the regulation of the secretory process in cells of the anterior pituitary gland. *J. Cell Biol.* 31:319–347.

Vaux, D., J. Tooze, and S. Fuller. 1990. Identification by anti-idiotype antibodies of an intracellular membrane protein that recognizes a mammalian endoplasmic reticulum retention signal. *Nature (Lond.).* 345:495–502.

Villa, A., A. H. Sharp, G. Racchetti, P. Podini, D. G. Bole, W. A. Dunn, T. Pozzan, S. H. Snyder, and J. Meldolesi. 1992. The endoplasmic reticulum of Purkinje neuron body and dendrites: molecular identity and specializations for Ca^{2+} transport. *Neuroscience.* 49:467–477.

Villa, A., P. Podini, M. C. Panzeri, H. D. Söling, P. Volpe, and J. Meldolesi. 1993*a*. The endoplasmic-sarcoplasmic reticulum of smooth muscle: immunocytochemistry of vas deferens fibers reveals specialized subcompartments differently equipped for the control of Ca^{2+} homeostasis. *J. Cell Biol.* 121:1041–1051.

Villa, A., P. Podini, A. Nori, M. C. Panzeri, A. Martini, J. Meldolesi, and P. Volpe. 1993*b*. The endoplasmic reticulum-sarcoplasmic reticulum connection. *Exp. Cell Res.* 209:140–148.

Volpe, P., B. H. Alderson-Lang, L. Madeddu, E. Damiani, J. H. Collins, and A. Margreth. 1990. Calsequestrin, a component of the inositol 1,4,5-trisphosphate-sensitive Ca^{2+} store of chicken cerebellum. *Neuron.* 5: 713–721.

Volpe, P., A. Martini, S. Furlan, and J. Meldolesi. 1994. Calsequestrin is a component of smooth muscles: the skeletal and cardiac muscle isoforms are both present, although in highly variable amounts and ratios. *Biochem. J.* 301:465–469.

Yaffe, D. 1968. Retention of differentiation potentialities during prolonged cultivation of myogenic cells. *Proc. Natl. Acad. Sci. USA.* 61:477–483.

Yaffe, D. 1973. Rat skeletal muscle cells. *In* Tissue Culture, Methods and Application II. Preparation of Primary Cultures. Academic Press, New York/London. 106–114.